

This article was downloaded by: [Tomsk State University of Control Systems and Radio]

On: 23 February 2013, At: 03:43

Publisher: Taylor & Francis

Informa Ltd Registered in England and Wales Registered Number: 1072954

Registered office: Mortimer House, 37-41 Mortimer Street, London W1T 3JH, UK



## Molecular Crystals and Liquid Crystals

Publication details, including instructions for authors and subscription information:

<http://www.tandfonline.com/loi/gmcl16>

### Proton Spin-Lattice Relaxation in the Critical Regime of a Nematic Liquid Crystal

S. K. Ghosh<sup>a</sup>, E. Tettamanti<sup>a</sup> & A. Panatta<sup>a</sup>

<sup>a</sup> Istituto di Fisica and Unità del GNSM del CNR, Università dell'Aquila, 67100, L'Aquila, Italy

Version of record first published: 20 Apr 2011.

To cite this article: S. K. Ghosh, E. Tettamanti & A. Panatta (1980): Proton Spin-Lattice Relaxation in the Critical Regime of a Nematic Liquid Crystal, *Molecular Crystals and Liquid Crystals*, 58:3-4, 161-178

To link to this article: <http://dx.doi.org/10.1080/00268948008082118>

PLEASE SCROLL DOWN FOR ARTICLE

Full terms and conditions of use: <http://www.tandfonline.com/page/terms-and-conditions>

This article may be used for research, teaching, and private study purposes. Any substantial or systematic reproduction, redistribution, reselling, loan, sub-licensing, systematic supply, or distribution in any form to anyone is expressly forbidden.

The publisher does not give any warranty express or implied or make any representation that the contents will be complete or accurate or up to date. The accuracy of any instructions, formulae, and drug doses should be independently verified with primary sources. The publisher shall not be liable for any loss, actions, claims, proceedings, demand, or costs or damages

whatsoever or howsoever caused arising directly or indirectly in connection with or arising out of the use of this material.

# Proton Spin-Lattice Relaxation in the Critical Regime of a Nematic Liquid Crystal

S. K. GHOSH, E. TETTAMANTI and A. PANATTA

*Istituto di Fisica and Unità del GNSM del CNR,  
Università dell'Aquila, 67100 L'Aquila, Italy*

(Received October 2, 1978; in final form June 19, 1979)

We present here the proton spin-lattice relaxation rates in MBBA measured over a large temperature range above the nematic-isotropic transition and at a number of frequencies. From the observed temperature and frequency dependences and using a recent theory, we demonstrate that these proton relaxation rates can be well understood when we consider:  $T_1^{-1}_{\text{expt}} = T_1^{-1}_{\text{CF}} + T_1^{-1}_0$ , where the first part arises from the critical fluctuations (CF) and the second from the diffusion-controlled mechanism(s). All the frequency dependence observed in the ranges of frequencies and temperatures measured is shown to arise from  $T_1^{-1}_{\text{CF}}$  which, according to the theory, consists of two parts— $T_1^{-1}_{\text{CF1}}$  and  $T_1^{-1}_{\text{CFN}}$ . Using the frequency dependences of these two parts, they are separated and compared with the theory. The agreement is reasonably good.

## I INTRODUCTION

Since the pioneering effort of Cabane and Clark<sup>1</sup> in relating <sup>14</sup>N line width in the critical regime of PAA with the Landau-de Gennes model<sup>2</sup> of the nematic-isotropic (N-I) transition, a number of reports<sup>3-8</sup> have appeared to understand the nuclear relaxation in this regime. All the authors are now in general agreement that the observed relaxation rates cannot all be attributed to the critical fluctuations (CF) as were done by Cabane and Clark. The role of the liquid-like behavior of nematics, which is present even in the ordered phase, in the relaxation processes cannot be underestimated. In fact, the contribution of this liquid-like behavior to the relaxation rates is not usually negligible even very close to the N-I transition temperature  $T_C$ . The general approach to understand the measured relaxation rates has been to divide into two parts:

$$T_1^{-1}_{\text{expt}} = T_1^{-1}_{\text{CF}} + T_1^{-1}_0 \quad (1)$$

The first part  $T_1)_{\text{CF}}^{-1}$  arises from the CF, while the second part  $T_1)_{\text{CF}}^{-1}$  from the liquid-like behavior mentioned above; the coupling between the CF and the liquid-like behavior is neglected. Assuming  $T_1)_{\text{CF}}^{-1}$  to be simple-liquid-like, two contrasting behaviors of  $T_1)_{\text{CF}}^{-1}$  have been observed,<sup>4,6-8</sup> particularly in different frequency regions. Both these contrasting behaviors of  $T_1)_{\text{CF}}^{-1}$  can be well understood by a recent theory,<sup>9</sup> according to which

$$T_1)_{\text{CF}}^{-1} = T_1)_{\text{CFN}}^{-1} + T_1)_{\text{CFL}}^{-1} \quad (2)$$

These two parts of CF are given by:

$$T_1)_{\text{CFN}}^{-1} = C_N \omega^{-1} x [(1 + x^2)^{-1} + 4(1 + 4x^2)^{-1}] \quad (3)$$

$$T_1)_{\text{CFL}}^{-1} = C_L T v^{1/2} \omega^{-1/2} y^{1/2} [(1 + \sqrt{1 + y^2})^{-1/2} + 4(1 + \sqrt{1 + 4y^2})^{-1/2}] \quad (4)$$

where  $x = \omega \tau_{\text{CFN}}$ ,  $y = \omega \tau_{\text{CFL}}$ ,  $C_N$  and  $C_L$  are constants independent of frequency  $\omega$  and temperature  $T$ , and  $v = v_0 \exp(W/T)$ , where  $v_0$  is also a constant and  $W$  is the activation energy of viscosity or molecular self-diffusion. The temperature dependences of the correlation times  $\tau_{\text{CFN}}$  and  $\tau_{\text{CFL}}$  are given by the Landau-de Gennes theory<sup>2,9</sup>

$$\tau_{\text{CFN}} = \tau_{\text{CFN}}^{(0)} \exp(W/T) (T - T^*)^{-\gamma} \quad (5)$$

$$\tau_{\text{CFL}} = \tau_{\text{CFL}}^{(0)} \exp(W/T) (T - T^*)^{-\gamma'} \quad (6)$$

where  $\gamma$  and  $\gamma'$  are the critical indices to be determined from experiments; both are equal to unity in a mean field theory like that of Maier and Saupe.<sup>10</sup> The temperature  $T^*$ , which is the apparent critical temperature for the isotropic-nematic transition, is slightly below  $T_C$  and is a parameter also to be determined from experiments. It is to be noted that  $T_1)_{\text{CFN}}$  arises from the  $\mathbf{q} = \mathbf{0}$  mode of the CF and  $T_1)_{\text{CFL}}$  from all other modes with  $\mathbf{q} \neq \mathbf{0}$ ;  $\tau_{\text{CFN}}$  and  $\tau_{\text{CFL}}$  are the correlation or the relaxation times of the modes with  $\mathbf{q} = \mathbf{0}$  and  $\mathbf{q} \rightarrow \mathbf{0}$ , respectively. The division of the CF into two distinct groups of modes and the consequent nonequivalence of  $\tau_{\text{CFN}}$  and  $\tau_{\text{CFL}}$  can be easily understood when one considers that the mode with  $\mathbf{q} = \mathbf{0}$  defines the system with no spatial inhomogeneity while the modes with  $\mathbf{q} \neq \mathbf{0}$  define the same with spatial inhomogeneity. Under such considerations, one can note that the mode with  $\mathbf{q} = \mathbf{0}$  can exist in a finite dimensional system while the modes with  $\mathbf{q} \neq \mathbf{0}$  cannot. In fact, under the rigorous framework of the Landau-de Gennes model, the mode with  $\mathbf{q} = \mathbf{0}$  cannot be treated even in the infinite dimensional system since the basic postulates of the model preclude the consideration of this mode which defines the equilibrium or the ground state of the system at  $T = T^*$ . Moreover, when we consider the modes with finite life times as in the Landau-de Gennes model, the ground state cannot be a pure state with  $\mathbf{q} = \mathbf{0}$  but will be a mixture of states with  $\mathbf{q} = \mathbf{0}$  and

$\mathbf{q} \neq 0$  as in the case of interacting boson system. Similar to the problem of interacting boson system, as in the case of Bose-Einstein condensation, we need to divide the CF into two distinct groups as above where the  $\mathbf{q} \rightarrow 0$  mode is not necessarily reducible to the  $\mathbf{q} = 0$  mode at the limit. From these and many other considerations, partly discussed in Ref. 9 and a more detailed discussion to appear elsewhere,<sup>11</sup> the separation of the CF into two distinct groups of modes with  $\mathbf{q} = 0$  and  $\mathbf{q} \neq 0$  seems well justified. From the experimental viewpoints, we shall demonstrate here that the proton spin-lattice relaxation rates in the critical regime, defined by the temperature range in which the correlation times of CF behave like expressions given by Eqs. (5) and (6), can be well understood by the above model of the CF.

## II EXPERIMENTAL

We measured proton spin-lattice relaxation rates in MBBA over a temperature range of 316.2–350°K ( $T_C \sim 316^\circ\text{K}$ ) at a number of frequencies (4, 5, 6, 8.8 and 20 MHz). These results are shown in Figure 1. Measurements of  $T_1$  were made by a modified version of the three-pulse method<sup>12</sup> which enabled us to obtain relative  $T_1$  at any frequency within a few parts in  $10^3$  and the absolute values within 1 %. Limitations of achieving higher accuracy were mainly from the considerations of experimental time and the consequent stability in the temperature control. During the measurement at any temperature, it was ensured that the sample temperature remained constant within  $\pm 0.1^\circ\text{K}$ . No appreciable temperature gradient was observed over the sample volume except at temperatures around  $T_C$  ( $\sim 0.2^\circ\text{K}$ ). The sample of MBBA used in the present measurements was commercial grade, distilled and degassed several times by standard techniques prior to sealing it under vacuum. All the data presented here were obtained with a single sample taking proper checks to ensure that the sample did not get deteriorated on the temperature cycling.

## III RESULTS AND DISCUSSIONS

Our directly measured proton spin-lattice relaxation rates  $T_1)_{\text{expt}}^{-1}$  at different temperatures and at different frequencies are shown in Figure 1. The following features of  $T_1)_{\text{expt}}^{-1}$  can be easily noticed in the figure:

- i) Fairly strong frequency dependence close to  $T_C$ ; the lower the frequency the higher the relaxation rate.
- ii) Diminishing frequency dependence with increasing temperature; within our experimental errors ( $\sim 1\%$ ), no observable frequency dependence

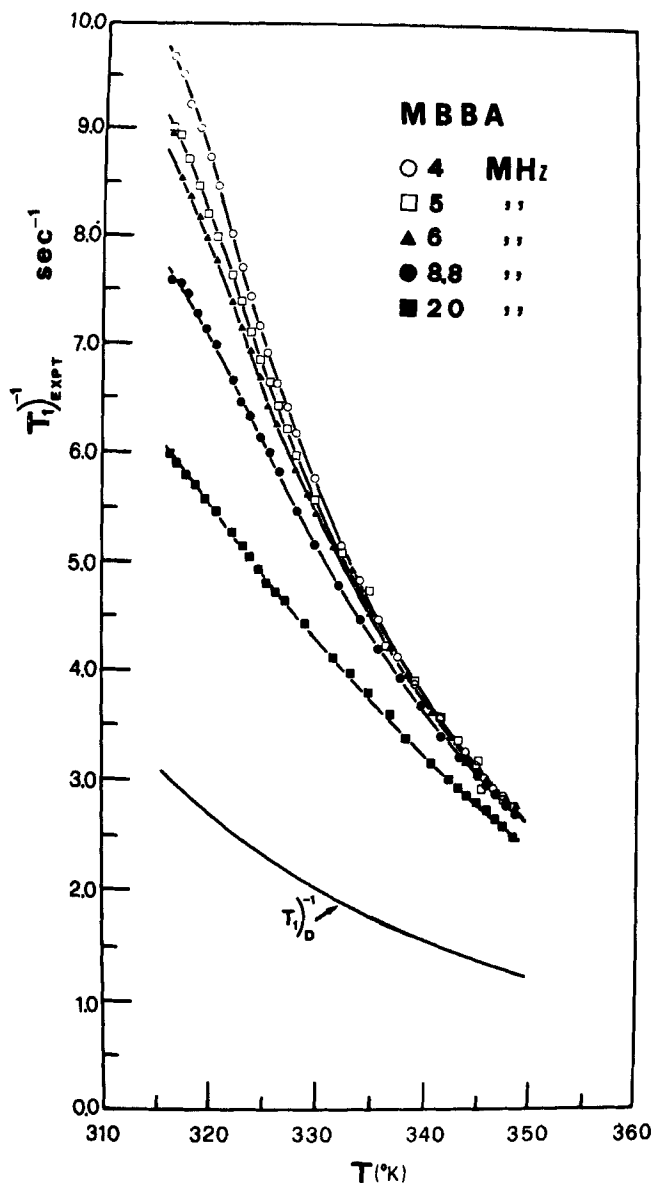


FIGURE 1 Proton spin-lattice relaxation rates  $T_1^{-1}$  in MBBA with the variation of temperature at different frequencies. The variation of  $T_1^{-1}_D$ , obtained from the low-temperature fit, is also included to show its relative weight on the observed relaxation rates. The solid lines are to aid eyes.

above about 340°K for the lowest three frequencies (4, 5 and 6 MHz) but not so with the other two frequencies (8.8 and 20 MHz) included.

iii) The lower the frequency the stronger the temperature dependence.

Looking at the point (i) alone, it might be tempting to attribute the observed frequency dependence to the diffusion-controlled intermolecular contribution.<sup>13,14</sup> In fact, the data at the lowest temperature measured ( $T = T_L = 316.2^\circ\text{K}$ ) can be well represented by the relation:

$$T_1)_{\text{expt}}^{-1} = E - F\omega^{1/2} \quad (7)$$

derived for isotropic liquids.<sup>13</sup> The constants  $E$  and  $F$  are independent of frequency but dependent on temperature and the coefficient of molecular self-diffusion  $D$ . The second term in Eq. (7) is a correction to the well-known BPP form for relaxation under "fast motion" approximation<sup>15</sup> represented by the first term  $E$ , and is expected to increase with decreasing  $D$  at any frequency. It is also well-known that the activation energy  $W$  obtained from the temperature dependence of  $E$  is the same as that for  $D$ . Under these simple considerations, we then expect the apparent  $W$  determined from the temperature dependence of  $T_1)_{\text{expt}}$  at any frequency to be lower than the actual one obtained from the direct measurements of  $D$ . Furthermore, the apparent  $W$  is expected to be closer to the actual one with the lowering of measuring frequency. In other words, we expect the difference between the apparent and actual  $W$  to decrease with decreasing frequency in the presence of this frequency dependent relaxation mechanism. On the contrary, the apparent  $W$  determined from high and low temperature data are all large in comparison to real  $W$  obtained from direct measurements of  $D$ ;<sup>16</sup> their differences decrease with increasing frequency. These observations suggest that the frequency-dependent diffusion-controlled intermolecular contribution<sup>13</sup> to the measured relaxation rates can be neglected in the ranges of frequencies and temperatures studied here.

Under the same considerations as above, we have assumed  $T_1)_0$  to be diffusion-controlled but independent of frequency. To emphasize this point, we shall henceforth denote  $T_1)_0$  by  $T_1)_D$  and write.<sup>15</sup>

$$T_1)_0^{-1} = T_1)_D^{-1} = K \exp\left(\frac{W}{T}\right) \quad (8)$$

where  $K$  is independent of  $T$  and  $\omega$ . Using this form of  $T_1)_0$ , we have determined both  $T_1)_{\text{CFL}}$  and  $T_{\text{CFN}}$  at different temperatures from  $T_1)_{\text{expt}}$  for various choices of  $T^*$ . The procedures followed in these determinations are described below briefly.

Considering the points (i) and (ii) together, particularly the frequency independence of  $T_1)_{\text{expt}}$  for the lowest three frequencies at high temperatures

and the simultaneously strong frequency dependence close to  $T_C$ , we can reasonably assume both  $x$  and  $y$  to be  $\gg 1$  for all our frequencies at  $T = T_L = 316.2^\circ\text{K}$ , the temperature closest to  $T_C$  measured (compare  $T_C \cong 316^\circ\text{K}$ ). At  $T = T_L$ , we then expect:

$$T_1)_{\text{expt}}^{-1} = A + B\omega^{-1/2} + C\omega^{-2} \quad (9)$$

The first term can be identified with the frequency independent  $T_1)_D^{-1}$ , the second with  $T_1)_{\text{CFL}}^{-1}$  for  $y \gg 1$ , and the third with  $T_1)_{\text{CFN}}^{-1}$  for  $x \gg 1$ , given by Eqs. (8), (4) and (3), respectively. For any frequency  $\omega$ , since  $T_1)_{\text{CFL}}^{-1}$  approaches its maximum while  $T_1)_{\text{CFN}}^{-1}$  to its minimum (zero) with  $T \rightarrow T^*$ , we assume further than the third term is negligible at  $T_L$ . Such an assumption may not be completely justified, particularly at lower frequencies, and may introduce some errors in determining  $A$  and  $B$  from the relation. In view of our earlier measurements in MBBA<sup>4</sup> at 14 and 60 MHz, where  $T_1)_{\text{CFL}}^{-1}$  were essentially incorporated in the diffusion term<sup>9</sup> or in  $T_1)_0^{-1}$ , and in view of experimental errors in absolute  $T_1)_{\text{expt}}$  ( $\sim 1\%$ ), we expect these errors in  $A$  and  $B$  not to be very serious. This is well supported by the excellent least squares fit (lsf) of our data at  $T = T_L = 316.2^\circ\text{K}$  to Eq. (9) without the third term. These results are shown in Figure 2.

As we have noted earlier, the constant  $A$  determined above yields  $T_1)_D^{-1}$  at  $T = 316.2^\circ\text{K}$ . Using this  $T_1)_D^{-1}$  and Eq. (8), we have obtained  $T_1)_D^{-1}$  at different temperatures with  $W = 3000^\circ\text{K}$  determined earlier from the direct measurements of  $D$ .<sup>16</sup> These  $T_1)_D^{-1}$  have been included in Figure 1 to point out that the observed  $T_1)_D^{-1}$  is an appreciable part of  $T_1)_{\text{expt}}^{-1}$  at any temperature and frequency used in our present measurements.

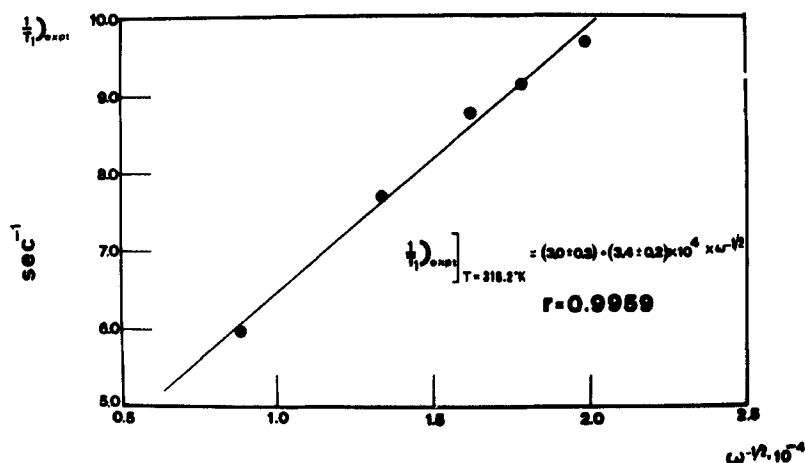


FIGURE 2 Least squares fit of  $T_1)_{\text{expt}}$  measured at  $316.2^\circ\text{K}$  and at different frequencies to Eq. (9), neglecting its third term. See the text for details.



Using Eq. (1) and  $T_1)_D^{-1}$  obtained as above,  $T_1)_CF^{-1}$  at different temperatures have been determined. These results together with  $T_1)_D^{-1}$  are shown in Figure 3. It can be noted here that the CF contribution to relaxation rates decreases fairly rapidly with increasing frequency at any temperature, while the other part  $T_1)_D^{-1}$  in the present case remains constant. Hence it is expected to determine  $T_1)_CF$  with higher precision with the lowering of frequency, if the relative experimental errors can be maintained the same. Furthermore, the purity of the sample is also expected to help considerably in obtaining  $T_1)_CF$  with higher precision. This latter conclusion we arrived at on comparing our present  $T_1)_\text{expt}$  with those obtained with a different sample and reported earlier.<sup>4</sup> These earlier 14 MHz data are almost coincident with our present 8.8 MHz data throughout the whole temperature range studied; the coincidence becomes closer with higher the temperature. These earlier data have not been included in Figure 1 to keep it legible. We are not certain about the nature or quantity of impurities in our present or earlier samples,

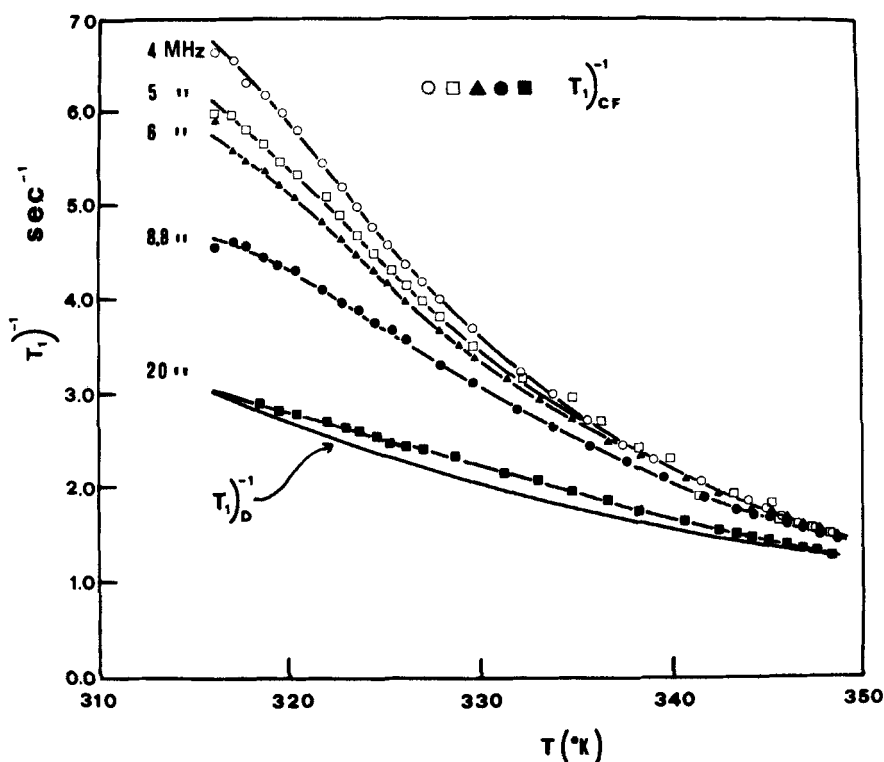


FIGURE 3  $T_1)_CF^{-1}$  versus  $T$  obtained at different frequencies subtracting  $T_1)_D^{-1}$  from  $T_1)_\text{expt}^{-1}$ . The plot of  $T_1)_D^{-1}$  versus  $T$  is also included to compare it with  $T_1)_CF^{-1}$  at different temperatures and frequencies. The solid lines are to aid eyes.

although both have identical  $T_C$  ( $\approx 316^\circ\text{K}$ ) within our experimental errors ( $\pm 0.2^\circ\text{K}$ ). But the present observation on relaxation rates suggests our earlier sample to be less pure than the present one, at least from the point of view of the proton relaxation rates.

We shall call the approximation under which Eq. (9) is obtained as the "slow motion" or the "low temperature" approximation. In contrast to this, we shall call the "fast motion" or the "high temperature" approximation where both  $x$  and  $y$  are  $\ll 1$ . Under this approximation,  $T_1)_{\text{CF}}$  becomes independent of frequency and can be written as:

$$T_1)_{\text{CF}}^{-1} = B'T(T - T^*)^{-1/2}\gamma' \exp \frac{W}{T} + C'(T - T^*)^{-\gamma} \exp \frac{W}{T} \quad (10)$$

where  $B'$  and  $C'$  are constants independent of  $T$  and  $\omega$ , and are related to  $B$  and  $C$  of Eq. (9), respectively. These relations can be easily obtained from Eqs. (3) and (4). The constants  $B'$  and  $C'$  have been determined for different fixed  $T^*$  ranging between  $315\text{--}316^\circ\text{K}$  at intervals of  $0.1^\circ\text{K}$  by the 1sf of frequency independent  $T_1)_{\text{CF}}$ , shown in Figure 3, to Eq. (10). In these fits, we have used  $\gamma = \gamma' = 1$ , taken from light scattering results.<sup>17,18</sup> One of these 1sf is shown in Figure 4. It is to be noted that the correlation coefficient  $r$  of these fits are not very good. This may be due to the particular choices of variables necessitated for the two-parameter fits. Considering the reproducibility of the data, the constants determined are reasonable. As we shall see shortly, a marked improvement of these fits is observed when  $\gamma$  is taken to be different from  $\gamma'$ . It is also to be noted that unrealistic results are obtained when the frequency independent  $T_1)_{\text{CF}}$  are fitted to any part,  $T_1)_{\text{CFL}}$  or  $T_1)_{\text{CFN}}$ . Similar unrealistic results are also obtained when the frequency independent  $T_1)_{\text{expt}}^{-1}$  are fitted to  $T_1)_{\text{D}}^{-1}$  with  $T_1)_{\text{CFL}}^{-1}$  or  $T_1)_{\text{CFN}}^{-1}$ .

Using  $B$  and  $B'$  determined from the low- and high-temperature fits, the constants  $C_L\nu_0^{1/2}$  and  $\tau_{\text{CFL}}^{(0)}$  have been determined. These constants are then used to determine  $T_1)_{\text{CFL}}$  and  $\tau_{\text{CFL}}$  at different temperatures, the former at different frequencies too (see Eqs. (4) and (6)). Using these  $T_1)_{\text{CFL}}$  and Eq. (2), we have determined  $T_1)_{\text{CFN}}$  at different temperatures and frequencies for each chosen  $T^*$ . One such set of  $T_1)_{\text{CFN}}$  is shown in Figure 5. Clear maxima of  $T_1)_{\text{CFN}}^{-1}$  at increasing temperatures with increasing frequency, as expected from Eqs. (3) and (5), can be noticed. Using  $x = 0.616$  for these maxima,  $\tau_{\text{CFN}}$  and the corresponding temperatures have been determined for each  $T^*$ ; the best 1sf of these data to Eq. (5), defined by the maximum  $r$ , has been obtained for  $T^* = 315.2^\circ\text{K}$ . These results are shown in Figure 6. It should be pointed out that we obtain here  $\gamma = 1.2$  instead of 1 used earlier for the high temperature fits. The high temperature fit for this particular  $T^*$  was redone with this value of  $\gamma$  in Eq. (10), and a marked improvement of the 1sf fit was observed as indicated by an increased  $r$  (from 0.95 to 0.98). These

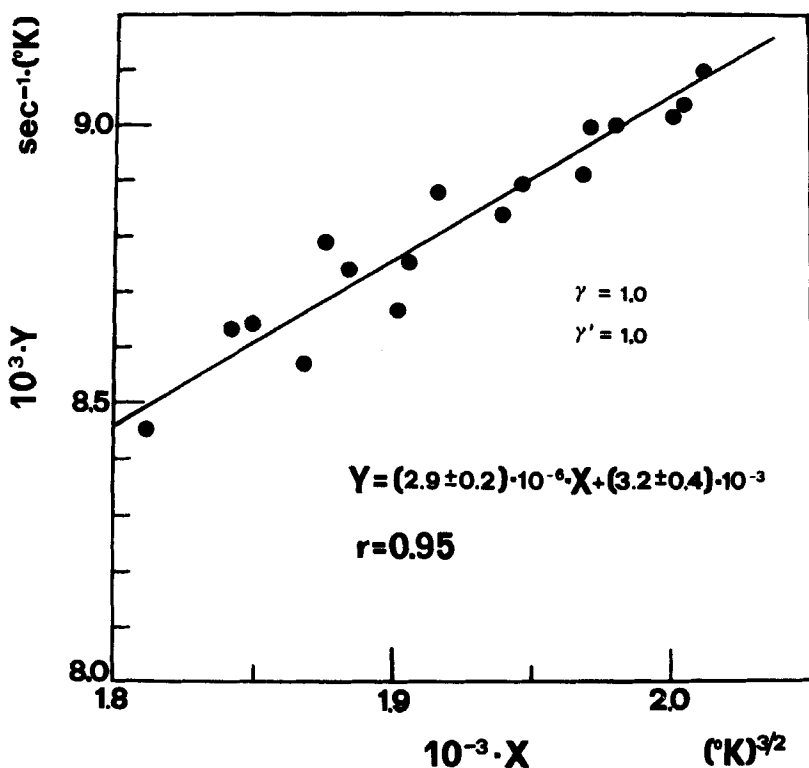


FIGURE 4 Least squares fit of the frequency independent  $T_1)_{CF}$  obtained at the lowest three frequencies (4, 5 and 6 MHz) to the relation:  $Y = B'X + C'$ , a rearranged form of Eq. (10) with  $Y = T_1)_{CF}^{-1} (T - T^*)_{\exp}(-W/T)$  and  $X = T(T - T^*)^{1/2}$ . We have used  $\gamma = \gamma' = 1$ ,  $W = 3000^\circ K$  and  $T^* = 315.2^\circ K$  for this particular fit.

results have not been included here for reasons noted below. Since the increase in  $T_1)_{CFL}^{-1}$  due to the parameter  $B'$  of the new fit remained within our estimated errors, no appreciable changes in either amplitudes or positions of the observed maxima of  $T_1)_{CFN}^{-1}$  were expected, and the procedure was not repeated for different  $T^*$  chosen. Corrections to  $T_1)_{CFN}^{-1}$  at different temperatures and frequencies due to this new fit have not also been made for the same reasons noted above.

It is clear from the above discussions and Figure 6 that our results are in fair agreement with the theoretical predictions<sup>9</sup> when the critical indices  $\gamma$  and  $\gamma'$  are taken to be different. The best fit values for  $\tau_{CFN}$  and  $\tau_{CFL}$  obtained from our measurements are:  $\tau_{CFN}^{(0)} = (2.5 \pm 0.6) 10^{-11}$  sec with  $\gamma = 1.2 \pm 0.1$ ,  $\tau_{CFL}^{(0)} = (1.2 \pm 0.2) 10^{-11}$  sec with  $\gamma' = 1$  (taken from the light scattering measurements),<sup>17/18</sup> for both,  $T^* = 315.2^\circ K$  and  $W = 3000^\circ K$  (obtained from the direct measurements of D).<sup>16</sup>

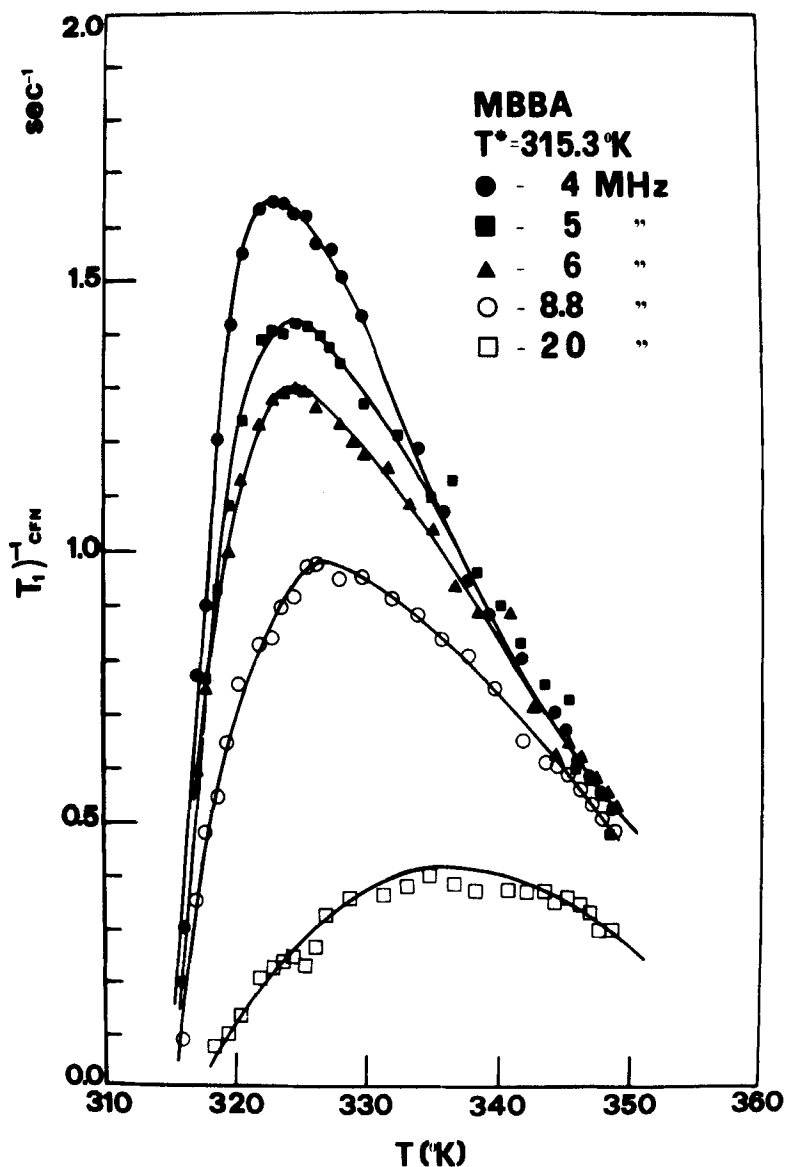


FIGURE 5 A typical set of  $(T_1)^{-1}_{\text{CFN}}$  with the variation of temperature obtained at different frequencies with  $T^* = 315.3^\circ\text{K}$  chosen. The solid lines are to aid eyes in locating the maxima.

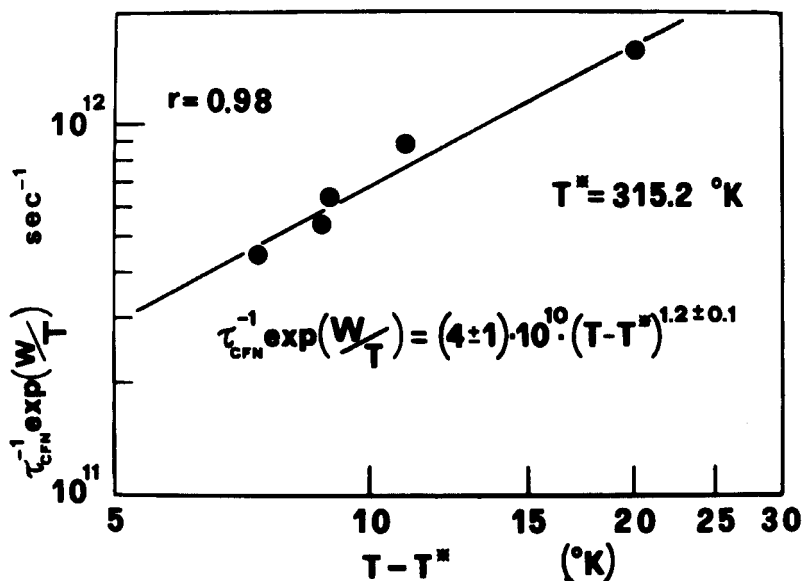


FIGURE 6 Log-log plot of  $\tau_{CFN}^{-1} \exp(W/T)$  versus  $T - T^*$  with  $T^* = 315.2^\circ\text{K}$  and  $W = 3000^\circ\text{K}$ . See text for details.

Some further checks on the theoretical predictions were also made. These are described below:

Using Eq. (3), the frequency dependence of the maximum of  $T_1)_{CFN}^{-1}$  or the minimum of  $T_1)_{CFN}$  can be written as

$$T_1)_{CFN}^{-1}(\text{max}) = T_1)_{CFN}^{\text{MIN}} = M\omega \quad (11)$$

where  $M$  is a constant independent of frequency. We show in Figure 7 the 1sf of  $T_1)_{CFN}^{\text{MIN}}$  obtained at different frequencies for  $T^* = 315.2^\circ\text{K}$  to Eq. (11). The agreement is fairly good in spite of different complex steps used to extract the data from directly measured relaxation rates. With the constant  $M$  thus determined and the best fit  $\tau_{CFN}$  obtained earlier and shown in Figure 6, we have also computed  $T_1)_{CFN}$  at different temperatures and frequencies with the help of Eq. (3). These results together with experimental data are shown in Figure 8(a); the agreement is reasonably good throughout the whole temperature range. In order to have a better appraisal of the estimated  $\gamma$ , similar comparisons as above have also been made for different values around 1.2; two of these sets of  $T_1)_{CFN}$  computed with  $\gamma = 1.1$  and 1 are shown together with the experimental data in Figure 8(b) and 8(c), respectively. It seems from such comparisons that the best agreement between the experiment and the theory is obtained for  $\gamma = 1.1$ , when the

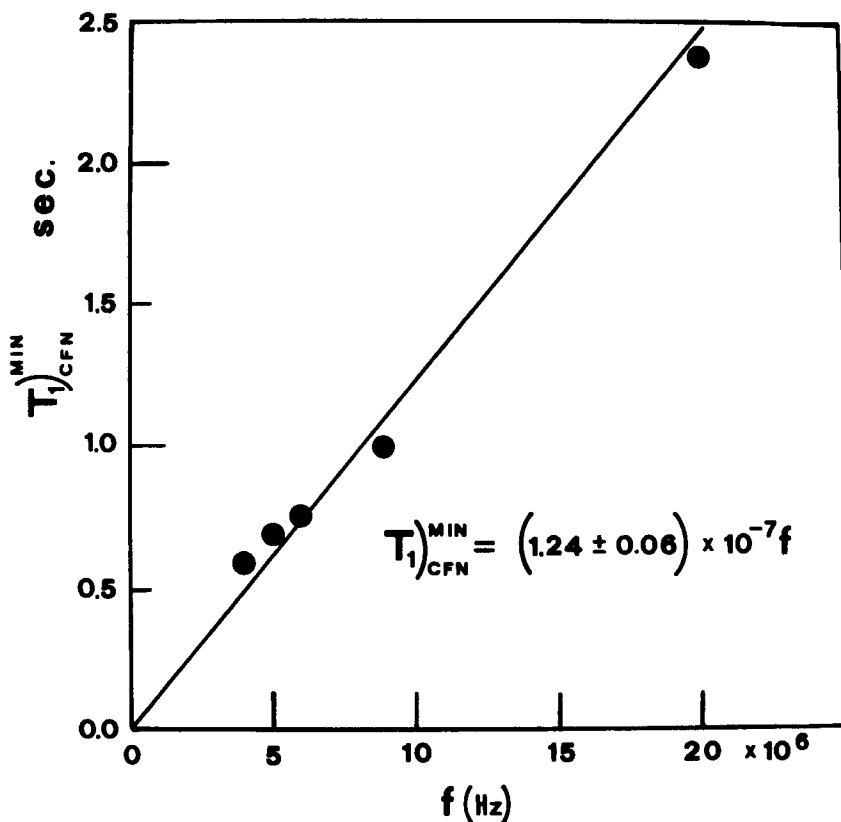


FIGURE 7  $T_1^{\text{MIN}}_{\text{CFN}}$  versus frequency  $f$  ( $=\omega/2\pi$ ). The straight line shows the least squares fit to Eq. (11).

whole temperature range of our measurements is considered. This value of  $\gamma$  is within our estimation obtained from the positions of the maxima of  $T_1^{\text{MIN}}_{\text{CFN}}$ . We refrain at this stage from making a more elaborate comparison between the theory and experiment, such as with the variation of other parameters like  $M$ ,  $\tau_{\text{CFN}}^{(0)}$  and  $\tau_{\text{CFL}}^{(0)}$ , since our data are not yet sufficiently comprehensive.

#### IV CONCLUSIONS

We have shown here that the proton relaxation rates in the critical regime of MBBA can be well understood when the observed relaxation rates are considered to consist of two parts—one arising from the CF of the order

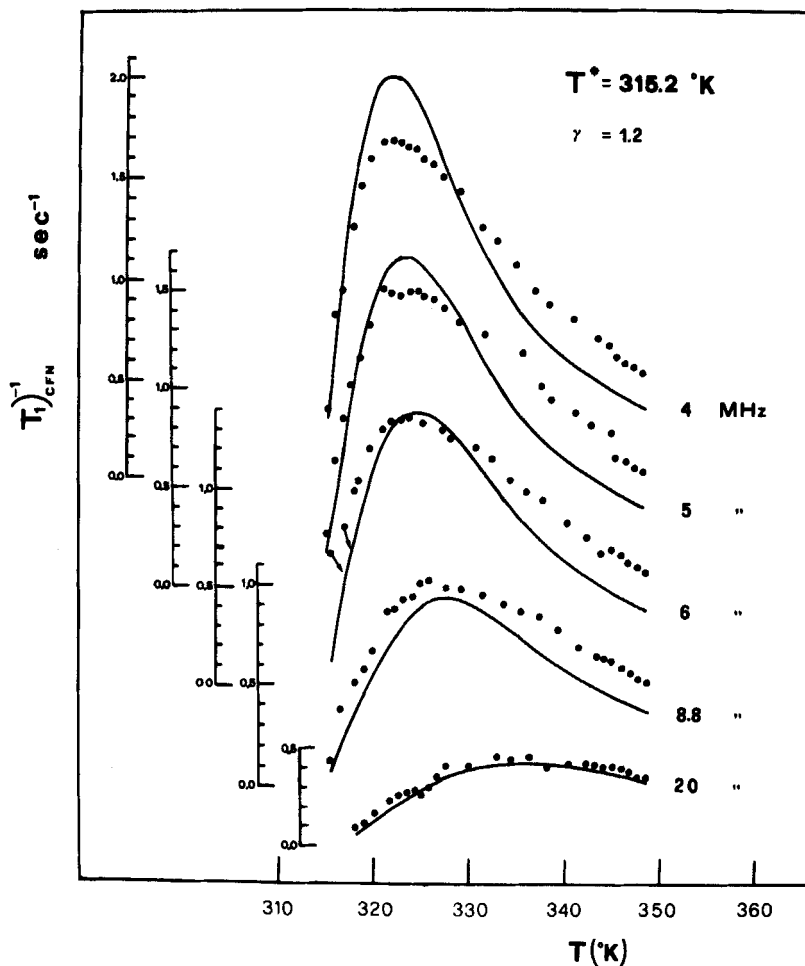


FIGURE 8(a) Comparison of  $(T_1)_{CFN}^{-1}$  obtained at different temperatures and frequencies with the theory. The solid lines are obtained from Eq. (3) using the necessary parameters determined by the least squares fits shown in Figures 6 and 7. The solid circles are experimental points similar to those shown in Figure 5 but obtained with  $T^* = 315.2^\circ\text{K}$ . See the text for details.

parameter and the other from the ordinary liquid-like behavior. In the range of frequencies studied here, the frequency dependence of relaxation rates is essentially determined by the former and not by the latter. Furthermore, our results confirm the necessity of separating the CF contribution into two parts as envisaged in a recent theoretical study<sup>9</sup> and also partially supported by some earlier experimental observations.<sup>3-8</sup> One part of this CF, which we denote here by  $(T_1)_{CFL}^{-1}$ , can be described by the standard Landau-de Gennes

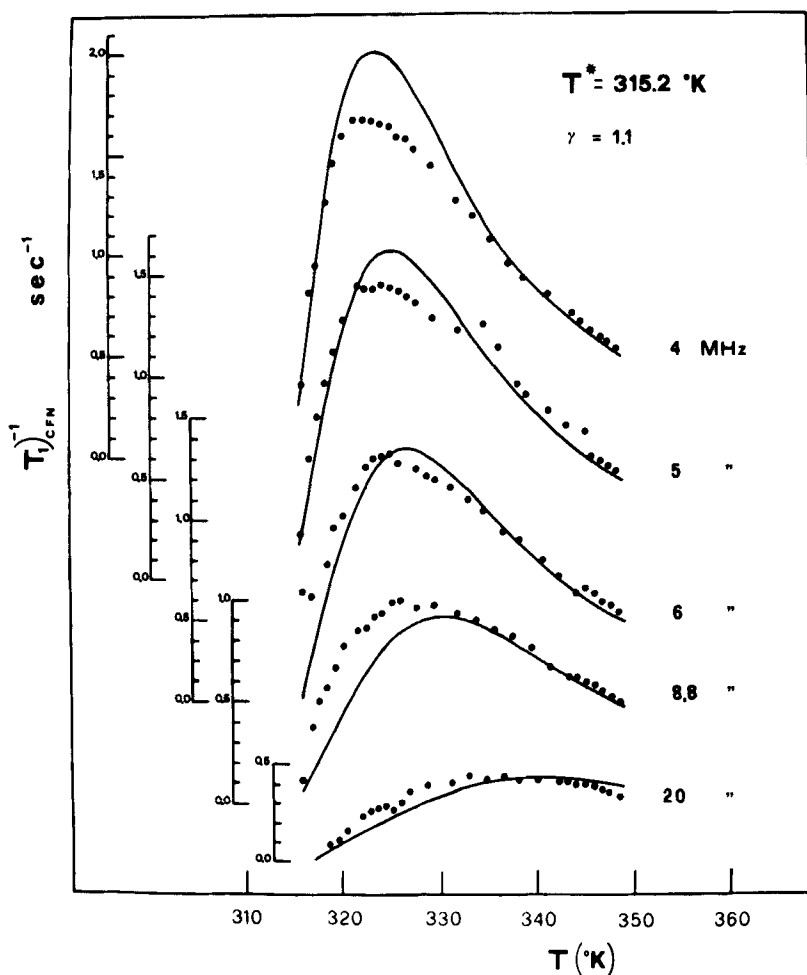
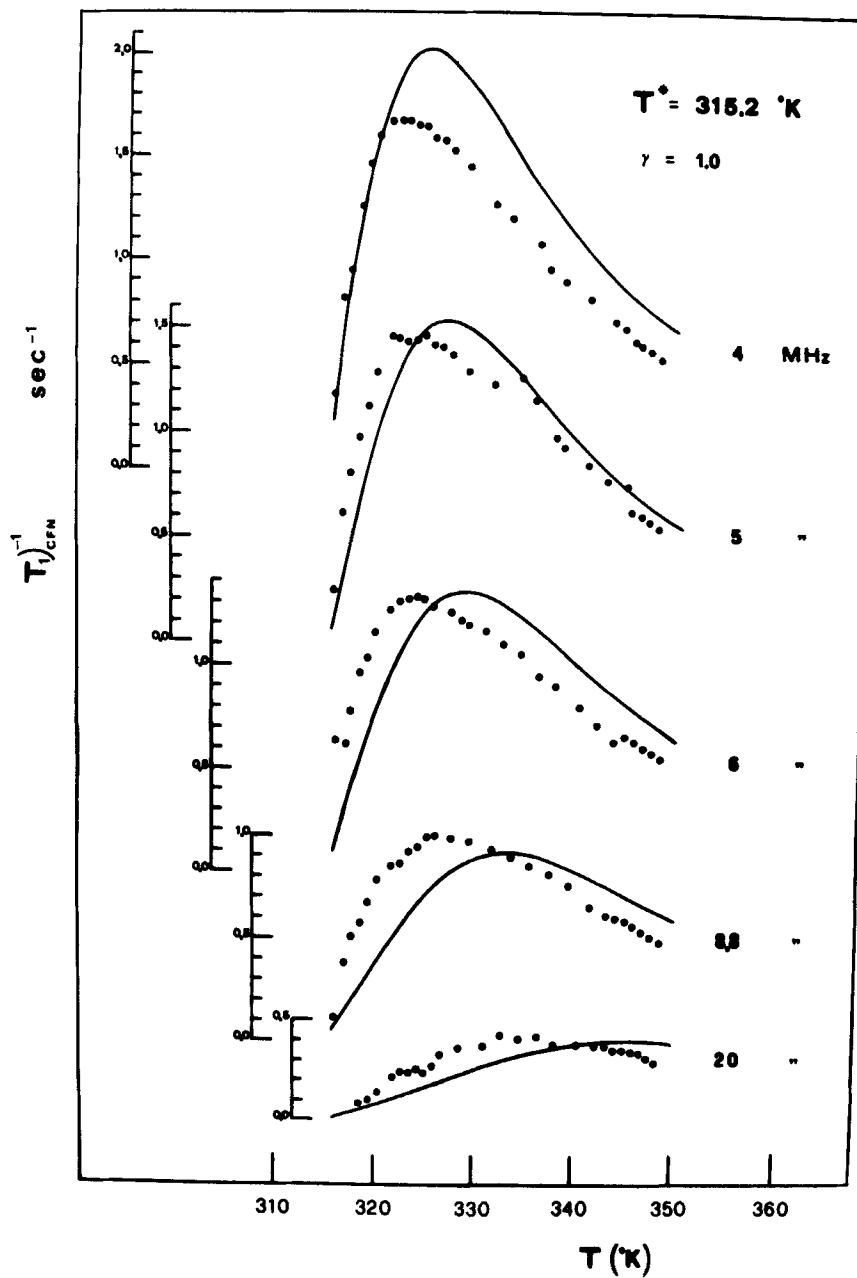


FIGURE 8(b) The same as Figure 8(a) except that the solid lines here are obtained with  $\gamma = 1.1$  from Eq. (3).

model<sup>2</sup> of the N-I transition. The other part, which was introduced in Ref. 9 for the first time and which we denote here by  $T_1)_{CFN}^{-1}$ , can be viewed as a necessary consequence of the basic postulates of the Landau-de Gennes model.<sup>11</sup> Our results on the proton relaxation rates in MBBA demonstrate clearly that none of  $T_1)_{CFL}^{-1}$  and  $T_1)_{CFN}^{-1}$  alone can explain the temperature and frequency dependences of the observed  $T_1)_{CF}^{-1}$ . It may be pointed out that the earlier efforts in separating the critical part from the directly measured relaxation rates, although partial and incomplete, were in the right directions. Observations on the frequency dependence of the relaxation rates are




 FIGURE 8(c) Similar to Figure 8 (b) with  $\gamma = 1.0$ .

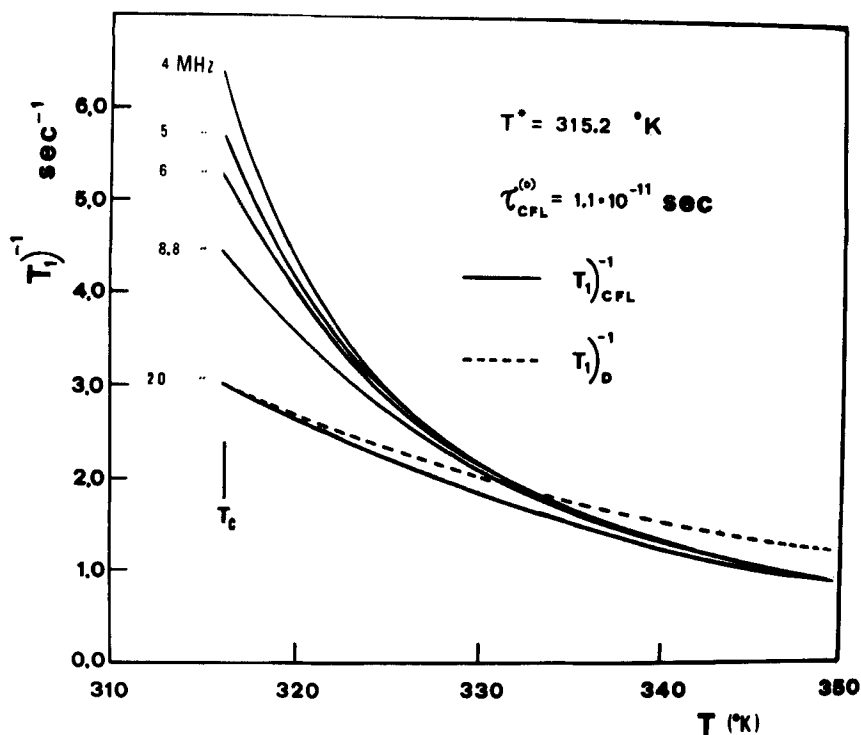


FIGURE 9 Shows the temperature dependence of  $T_1^{-1}_{CFL}$  at different frequencies obtained with the use of Eq. (4) and the necessary parameters determined from the low- and high-temperature fits given in Figures 3 and 5. The plot of  $T_1^{-1}_D$  versus  $T$  is also included in the figure to show that its behavior is very close to that of  $T_1^{-1}_{CFL}$  versus  $T$  at higher frequencies.

very essential for a complete separation of the different contributions. Some of the problems of such separation have been noted earlier. Here we like to point out that  $T_1^{-1}_{CFL}$  may be fairly closely approximated to diffusion-like, as has essentially been done in our earlier study,<sup>4</sup> in a certain frequency range. This can be easily noted in Figure 9 where we have shown  $T_1^{-1}_{CFL}$  determined at different temperatures and frequencies together with the frequency-independent but diffusion-controlled  $T_1^{-1}_D$ .

We would like to make some comments on the discrepancy observed between our  $\tau_{CFL}$  and those obtained by the two different light scattering experiments.<sup>17,18</sup> For a meaningful comparison, we have also computed  $\tau_{CFL}^{(0)}$  from light scattering results with  $W = 3000^\circ\text{K}$  and  $T^*$  as reported. These are  $3.5 \times 10^{-11}$  and  $4.8 \times 10^{-11}$  sec obtained from Refs. 17 and 18, respectively. A factor of two in discrepancy between NMR and light scattering results can be easily accounted for when one considers that the

Landau-de Gennes theory predicts in fact the nondiagonal components of the order parameter tensor  $\bar{Q}$  to decay twice faster than the diagonal ones. Furthermore, the local-field effects,<sup>2c</sup> which play a considerable role in the optical but not in the NMR results, need some special mention in this connection. It is well-known that the macroscopic and microscopic  $\bar{Q}$  are not strictly proportional, as has also been stressed recently by Hansen and Shen,<sup>19</sup> because of the local-field effects. There exist also a number of simplifying assumptions in applying the theory to the real system like MBBA. It is not clear how all these contribute to the observed discrepancy.

Finally, to conclude, we would like to note that a more elaborate comparison between the theory and the experiment than the one presented here could be achieved most conveniently by measuring the relaxation rates at larger number of frequencies. Particular interest will be in making such measurements using dilution technique to separate the contributions from intra- and intermolecular dipole pairs.

### Acknowledgments

The authors take great pleasure in thanking Dr. P. L. Indovina of the Istituto Superiore di Sanità, Rome, for his participation in the earlier phase of this work and also for his help in preparing the samples used in these studies.

### References

1. B. Cabane and W. G. Clark, *Phys. Rev. Lett.*, **25**, 91 (1970).
2. P. G. de Gennes, (a) *Phys. Lett.*, **30A**, 454 (1969), (b) *Mol. Cryst. Liquid Cryst.*, **12**, 193 (1971), and (c) *The Physics of Liquid Crystals* (Oxford, 1974).
3. R. Y. Dong, W. F. Forbes, and M. M. Pinar, *J. Chem. Phys.*, **55**, 145 (1971).
4. S. K. Ghosh, E. Tettamanti, and P. L. Indovina, *Phys. Rev. Lett.*, **29**, 638 (1972).
5. B. Cabane, *Adv. Mol. Relaxation Process*, **3**, 341 (1972).
6. R. Y. Dong, M. Wisniewska, E. Tomchuk, and E. Bock, *Canad. J. Phys.*, **52**, 766 (1974).
7. R. Y. Dong, E. Tomchuk, and E. Bock, *Canad. J. Phys.*, **53**, 610 (1975).
8. S. K. Ghosh, E. Tettamanti, and P. L. Indovina, *Z. Phys.* **24B**, 227 (1976).
9. S. K. Ghosh, in *Local Properties at Phase Transitions*, edited by K. A. Muller and A. Rigamonti (Course LIX, International School of Physics "Enrico Fermi", North-Holland, 1976), p. 730.
10. W. Maier and A. Saupe, *Z. Naturforsch.*, **15a**, 287 (1960).
11. S. K. Ghosh, E. Tettamanti, and A. Panatta, to be published.
12. T. Ghose, S. K. Ghosh, and D. K. Ray, *Nuovo Cimento*, **5**, 1771 (1957); S. K. Ghosh, E. Tettamanti, and A. Panatta, to be published.
13. J. F. Harmon and B. H. Muller, *Phys. Rev.*, **182**, 400 (1969).
14. M. Vilfan, R. Blinc, and J. W. Doane, *Solid State Commun.*, **11**, 1073 (1972).
15. A. Abragam, *The Principles of Nuclear Magnetism* (Oxford, 1961).
16. S. K. Ghosh and E. Tettamanti, *Phys. Lett.*, **43A**, 361 (1973).
17. T. W. Stinson III and J. D. Litster, *Phys. Rev. Lett.*, **25**, 503 (1970).
18. G. K. L. Wong and Y. R. Shen, *Phys. Rev. Lett.*, **30**, 895 (1973).
19. E. G. Hanson and Y. R. Shen, *Mol. Cryst. Liq. Cryst.*, **36**, 193 (1976).

